

## OZONE VARIATION IN THE SOUTHERN POLAR STRATOSPHERE

Hartwig GERNANDT<sup>1</sup>, Andreas HERBER<sup>1</sup>, Peter VON DER GATHEN<sup>1</sup>  
and Susumu KANETO<sup>2</sup>

<sup>1</sup> *Alfred Wegener Institute for Polar and Marine Research, Research Unit Potsdam,  
Telegrafenberg A 43, D-14473 Potsdam, Germany*

<sup>2</sup> *Japan Meteorological Agency, Ote-machi 1-chome, Chiyoda-ku, Tokyo 100-8122*

**Abstract:** The objective of this study is to discuss the altitude dependent inter-annual variability of ozone inside the southern polar stratospheric vortex during spring. Trend of ozone mixing ratio as well as possible correlation to global forcing processes, and transient perturbations by volcanic aerosols are obtained by using balloon-borne ozone sonde data obtained at three Antarctic stations located at about 70°S between 30°E and 08°W.

For the period 1966 to 1995 negative trend in ozone mixing ratio is statistically significant with 99% confidence between the 330 K and 670 K isentropic level. For the period 1985 to 1995 significant negative trends are recognized in three altitude ranges during spring.

The interannual variability of ozone in the middle polar stratosphere is strongly affected by the El Nino Southern Oscillation (ENSO). For the period from 1985 to 1988 the pattern of year to year changes might be explained by a synergetic effect of ENSO and Quasi Biennial Oscillation of winds in the tropical stratosphere. Inside the polar vortex the impact of volcanic aerosols on vertical ozone distribution shows a similar altitude dependency as found for mid-latitudes but downward displaced by about 5 km in altitude. In the lowest part of the polar stratosphere ozone is additionally removed when volcanic aerosol loading is extremely high.

The intercomparison of balloon-borne ozone observations from Arctic and Antarctic stations shows significant differences in the recent mean annual pattern but also similarities in the seasonal behaviour.

### 1. Introduction

In the Antarctic environment the stratosphere is the highest atmospheric region where signals of a changing atmosphere were clearly detected since the 1980's. During spring season significant ozone loss is mainly addressed to an anthropogenic perturbation on atmospheric chemical processes inside the dominating stratospheric vortex circulation (WMO, 1991, 1994). Because ozone is transported from the tropical stratosphere towards polar latitudes, its spatial distribution as well as temporal variation in the polar region strongly depends on global atmospheric processes. The correlation between temperatures in the lower stratosphere and total ozone column density was discussed in detail by RANDEL and COBB (1994) and for southern polar latitudes by CHUBACHI (1993). But correlation signals as well as telecommunication patterns were reported between ozone column densities at mid and subpolar latitudes and the solar

cycle (ANGLE, 1988, 1989; HOOD and McCORMACK, 1992), the Quasi-Biennial Oscillation (QBO) (HASEBE, 1980; LABITZKE, 1987; BOWMAN, 1989; VAN LOON and LABITZKE, 1990; GRUZDEV and MOKHOV, 1992), and the El Nino Southern Oscillation (ENSO) (SHIOTANI, 1992; ZEREFOS *et al.*, 1992).

Beside this quasi periodic forcing transient perturbations such as strong sulphate aerosol loading into the stratosphere after volcanic eruptions may also have significant impact on the spatial and temporal ozone distributions in the stratosphere. After the eruptions of Mt. Pinatubo and Cerro Hudson in 1991, the impact of volcanic aerosols on stratospheric ozone was studied by JOHNSON *et al.* (1995), ANSMANN *et al.* (1996) and modelled by TIE *et al.* (1994) and SOLOMON *et al.* (1996) for mid and subpolar latitudes. Even in the lowest part of the southern polar stratosphere a strong ozone removal was recorded at South Pole Station in October for the years 1992 to 1994 when volcanic aerosols resided there (HOFMANN and OLTMANS, 1993; HOFMANN *et al.*, 1994, 1995). Similar ozone losses were found at Neumayer Station ( $70^{\circ}\text{S}$ ,  $8^{\circ}\text{W}$ ) and even in the lower Arctic stratosphere above Ny-Ålesund Station ( $79^{\circ}\text{N}$ ,  $12^{\circ}\text{E}$ ) (GERNANDT *et al.*, 1996).

For mid and subpolar latitudes long-term negative trends of ozone column densities were identified by using ground-based and satellite observations in a global scale (BOJKOV and FIOLETOV, 1995; STOLARSKI *et al.*, 1992). They are stronger in higher latitudes during winter and spring months. Altitude dependent negative trends retrieved from ozone sonde and lidar observations were reported for mid latitudes by CLAUDE *et al.* (1994). For upper stratospheric altitudes negative trends were obtained for zonally averaged ozone amount retrieved from SBUV satellite observations (HOOD and McCORMACK, 1992; HOLLANDSWORTH *et al.*, 1995). They are strongest at subpolar latitudes during fall and early winter, and might also be associated with the enhanced levels of chlorine and bromine and, hence, increasing removal of ozone by gas phase chemical reactions at those altitudes (HOOD *et al.*, 1993).

Since the 1980's in the southern polar stratosphere an increasing ozone loss has occurred in September and October each year. Its growing horizontal extension has been recorded by TOMS within the stratospheric vortex since 1979 (WMO, 1991, 1994). This chemical removal of ozone is caused by heterogeneous activation of reactive halogen species, such as chlorine, at the surface of polar stratospheric cloud (PSC) particles (SOLOMON, 1990). The formation and existence of PSCs depend on stratospheric temperatures during winter and spring. So the meteorological conditions in the polar stratosphere control those chemical processes removing ozone.

So far quite few studies are referred to the altitude dependence of these processes based on observations with sufficient vertical resolution with respect to the lower and middle stratosphere inside the southern polar vortex. For tropospheric and stratospheric altitudes the vertical ozone distribution can be studied in more detail by using balloon-borne ozone sonde records. These *in-situ* observations provide the vertical ozone distribution up to approximately 30 km altitude even during polar night conditions. At about  $70^{\circ}\text{S}$  latitude ozone sonde measurements are available from three Antarctic stations, *i.e.* Syowa Station ( $69^{\circ}\text{S}$ ,  $39^{\circ}\text{E}$ ), Georg Forster Station ( $71^{\circ}\text{S}$ ,  $12^{\circ}\text{E}$ ), and Neumayer Station ( $70^{\circ}\text{S}$ ,  $08^{\circ}\text{W}$ ). The mean annual patterns of the vertical distribution of ozone concentration retrieved from balloon observations for periods 1967 to 1979 and 1980 to 1984 at Syowa, 1985 to 1991 at Georg Forster, and 1992 to 1995 at

Neumayer were discussed in detail by GERNANDT *et al.* (1996) showing the temporal and vertical development of the spring ozone minimum at 70°S. Since 1980 this minimum has appeared in late winter and spring as shown by the Syowa ozone sonde records (CHUBACHI, 1984). So far this alteration has been the strongest and clearest signal for a long-term change in the southern polar atmosphere.

The objective of this study is to analyse the altitude dependent interannual variability of ozone inside the southern stratospheric polar vortex during the spring season. The focus is to retrieve altitude dependent trends as well as to discuss possible teleconnections of polar stratospheric ozone variation to global atmospheric processes and to transient perturbations by volcanic aerosols. Finally, balloon-borne ozone sonde observations from the Antarctica and Arctic are briefly discussed in order to show some features of ozone variability for both polar regions in a climatological time scale.

## 2. Data Records and Multiple Linear Regression

The Stations Syowa (SY), Georg Forster (GF), and Neumayer (NM) are located near 70°S between 8°W and 39°E. Regular balloon-borne observations at these locations provide ozone and temperature data from inside of the stratospheric polar vortex which exists from May through November each year. As the focus is the altitude dependent long-term interannual variability during the ozone minimum in September and October, all available balloon-borne measurements performed at these three sites have been considered to calculate appropriate mean profiles of ozone mixing ratio by volume (ppm). As suggested in Table 1 data records for two independent time series are available for time intervals of about 30 years and 10 years, respectively.

Mesoscale advective processes as well as adiabatic vertical motions may influence the vertical ozone distribution. In order to reduce those effects for the interannual analysis, appropriate seasonal or monthly means of ozone mixing ratios were calculated for isentropic levels of potential temperature with steps of 10 K. So quasi conservative values are adopted for ozone as well as for the altitude coordinate in this study.

Syowa data for September and October are used to calculate the mean vertical ozone distribution between the isentropic levels of 310 K (approximately 6 km) and about 700 K (approximately 25 km); hereafter referred to as time series SY (spring). Although there are temporal gaps in the years from 1966 to 1987, this time series might be useful to estimate the altitude dependent long-term trends of stratospheric ozone inside the polar vortex for spring season. As a second contingent time series the balloon-borne soundings of the Georg Forster and Neumayer Station both located at 70°S with a longitudinal difference of about 20° are used for the period 1985 to 1995, *i.e.* roughly covering one solar cycle. Monthly means were calculated for October between the isentropic levels of 310 K and about 850 K (approximately 30 km). These data are referred to as time series GFNM (October) for a 11 years period with consistent and equidistant data when lowest stratospheric ozone content occurs. GFNM (October) data are used to study the trend for a shorter time interval as well as the additional variance of ozone modified by the total column density of sulphate aerosols in the polar stratosphere and the relative phase of quasi internal and external forcing phenomena as the QBO of stratospheric winds in the tropical stratosphere, the

Table 1. Sounding statistics; Syowa Station (SY) for September and October; Georg Forster Station (GF) and Neumayer Station (NM) for October.

Year	SY (69°S, 39°E) September and October time series SY (spring)	GF (71°S, 12°E) October time series GFNM (October)	NM (70°S, 08°W) October
1966	5/ 3 (700 K)		
1967			
1968	6/ 3 (700 K)		
1969			
1970			
1971	15/ 9 (700 K)		
1972	5/ 3 (660 K)		
1973			
1974	6/ 3 (700 K)		
1975	3/ 3 (670 K)		
1976			
1977			
1978			
1979			
1980			
1982			
1983	7/ 7 (700 K)		
1984	4/ 4 (700 K)		
1985		15/3 (1000 K)	
1986		5/3 (1000 K)	
1987	10/ 9 (700 K)	10/2 ( 880 K)	
1988	8/ 8 (700 K)	8/7 (1000 K)	
1989	6/ 5 (700 K)	3/2 (1000 K)	
1990	11/10 (700 K)	7/3 (1000 K)	
1991	7/ 6 (700 K)	6/3 (1000 K)	
1992	9/ 7 (700 K)		8/8 ( 840 K)
1993	10/10 (700 K)		6/3 (1000 K)
1994	12/11 (700 K)		5/4 (1000 K)
1995	9/ 9 (700 K)		8/3 (1000 K)

$x/y$  ( $z$ ):  $x$  is number of contributing soundings at 310 K,  $y$  is number of contributing soundings at the upper isentropic level ( $z$ ).

solar activity and the ENSO. Mean values of these independent variables are used according to the time series SY (spring) given in Table 2 and GFNM (October) given in Table 3. QBO means of tropical stratospheric winds are taken for the 15 hPa level as obtained from radiosonde measurements at Singapore (1°N, 104°E). Solar cycle variations in the UV spectral range are highly correlated with the 10.7 cm solar radio flux ( $\text{W m}^{-2} \text{Hz}^{-1}$ ). This solar radio flux regularly observed at Ottawa till 1991 and then at Penticton is used as an intensity index of the solar UV. A dimensionless index value is obtained by multiplying the 10.7 cm radio flux value by  $10^{23} \text{W}^{-1} \text{m}^2 \text{Hz}$ . ENSO

Table 2. Forcing parameters as used for the SY (spring) record from 1966 to 1995 and from 1987 to 1995.

Year	QBO (15 hPa) (m/s)	ENSO (normalized SOI index)	SUN (10.7 cm flux index)	$AE_{tot}$ (65°S–75°S) ( $\mu\text{m}^2/\text{cm}^2$ )
1966	09.63	-0.29	1097.5	
1968	-20.55	-0.37	1467.5	
1971	11.85	1.68	1056.0	
1972	-23.03	-1.33	1173.5	
1974	-15.78	0.95	927.0	
1975	11.35	1.93	776.5	
1983	07.50	0.62	1107.0	
1984	-28.23	-0.23	758.0	
1987	05.25	-0.95	921.0	24.67
1988	09.78	1.65	1611.5	22.36
1989	-19.00	0.74	2173.0	22.21
1990	10.10	-0.49	1797.0	19.49
1991	-06.98	-1.67	1909.5	93.87
1992	-14.83	-1.05	1238.0	201.45
1993	09.28	-1.19	936.5	94.27
1994	-27.60	-1.70	834.0	40.03
1995	08.28	0.03	749.5	32.00

September–October means for QBO at 15 hPa, for normalized Southern Oscillation index (SOI), for 10.7 cm radio flux index (SUN) as a proxy indicator for solar UV radiation, and for zonally averaged stratospheric aerosol surface column density ( $AE_{tot}$ ) between 65°S and 75°S.

Table 3. Same as Table 2 for the GFNM (October) record from 1985 to 1995 (October mean).

Year	QBO (15 hPa) (m/s)	ENSO (normalized SOI index)	SUN (10.7 cm flux index)	$AE_{tot}$ (65°S–75°S) ( $\mu\text{m}^2/\text{cm}^2$ )
1985	-1.5	-0.82	747	25.84
1986	-34.4	0.66	830	23.40
1987	13.9	-0.72	981	25.45
1988	-37.1	1.37	1698	24.40
1989	1.2	0.62	2087	21.55
1990	10.3	-0.15	1820	20.01
1991	-28.8	-1.66	2013	104.46
1992	16.2	-2.17	1308	176.77
1993	-34.0	-1.55	1003	93.85
1994	14.3	-1.65	877	39.87
1995	-21.6	-0.34	779	25.00

is considered by a monthly normalized Southern Oscillation Index (SOI) derived from the normalized surface pressure difference between Tahiti and Darwin (Australia). The stratospheric aerosol loading is included by zonally averaged monthly means of total aerosol surface column densities between 65°S and 75°S retrieved from the altitude integrated surface area density profiles measured by the SAGE II satellite instrument.

According to the GFNM (October) ozone data monthly means were calculated for October of the period 1985 to 1995.

A simple multiple least square fitting method is used to calculate the linear regression coefficients ( $m_{n,i}$ ) between observed mean ozone mixing ratios ( $\text{MO3}_i$ ) and the independent forcing variables at the individual isentropic levels ( $i$ ).

$$\text{MO3}_i = m_{1,i} \times T + m_{2,i} \times Q + m_{3,i} \times E + m_{4,i} \times S + m_{5,i} \times AE_{\text{tot}} + B_i. \quad (1)$$

$\text{MO3}_i$  is the corresponding time series of observed mean ozone mixing ratios by volume (ppm) at the isentropic level  $i$  according to Table 1. The potential temperature steps are 10 K. The independent variables are time ( $T$ ) as well as corresponding means (Tables 2 and 3) for the solar 10.7 cm radio flux index ( $S$ ), QBO at 15 hPa ( $Q$ ), ENSO Index ( $E$ ), and zonally averaged stratospheric aerosol surface column densities ( $AE_{\text{tot}}$ ).  $B_i$  is the residual ozone mixing ratio.

The regression coefficients ( $m_{n,i}$ ) yield the altitude dependent correlation between ozone mixing ratio and the considered independent forcing variables. They are

$m_{1,i}$ : coefficient for time trend (ppm/year),

$m_{2,i}$ : coefficient for QBO forcing (ppm/ $\text{ms}^{-1}$ ),

$m_{3,i}$ : coefficient for ENSO forcing (ppm/SOI index),

$m_{4,i}$ : coefficient for solar cycle forcing (ppm/flux index),

$m_{5,i}$ : coefficient for stratospheric aerosol forcing (ppm/ $\mu\text{m}^2 \text{cm}^{-2}$ ).

The statistical significance (95% confidence level) of the multiple correlation between  $\text{MO3}_i$  and forcing variables is checked by the Fisher test (TAUBENHEIM, 1969). The  $F$ -parameter and  $r^2$  for the regression between observed  $\text{MO3}_i$  and ozone values obtained by using eq. (1) are calculated for each isentropic level ( $i$ ). The statistical confidence of partial correlations for each  $m_{n,i}$  is checked by the Students  $t$ -distribution test (TAUBENHEIM, 1969). The  $t$  value is obtained by  $t = m_{n,i}/sm_{n,i}$ , where  $sm_{n,i}$  is the standard deviation of the corresponding regression coefficient  $m_{n,i}$ .

Several model runs according to eq. (1) have been performed for different time intervals and different groupings of the independent variables  $T$ ,  $Q$ ,  $E$ ,  $S$ , and  $AE_{\text{tot}}$ : (a) for SY (spring) with  $T$ ,  $Q$ ,  $E$ , and  $S$  for the time interval 1966 to 1995; (b) for SY (spring) with  $T$ ,  $Q$ ,  $E$ ,  $S$ , and  $AE_{\text{tot}}$  for the time interval 1987 to 1995; (c) for GFNM (October) with  $T$ ,  $Q$ ,  $E$ , and  $S$ , and (d) for GFNM (October) with  $T$ ,  $Q$ ,  $E$ ,  $S$ , and  $AE_{\text{tot}}$  both for the time interval 1985 to 1995.

In Fig. 1 the profiles of the correlation value  $r^2$  are shown for the regression calculations according to eq. (1). For calculation (a), *i.e.*: SY (spring) from 1966 to 1995, the 95% confidence is obtained between 340 K and 650 K (Fig. 1a). For the shorter period from 1987 to 1995, *i.e.* calculation (b), the 95% confidence is only obtained close to 400 K and 600 K, respectively. For GFNM (October) the regression became better for calculation (d) when all independent variables including  $AE_{\text{tot}}$  are considered (Fig. 1b). However the 95% confidence is only obtained at altitude ranges close to 370 K, 430 K, 530 K, and 800 K. No significant correlation is found at altitudes around 620 K.

Additionally for the same period of years daily radiosonde temperature data are used which were recorded at NM from May through October for the years from 1985

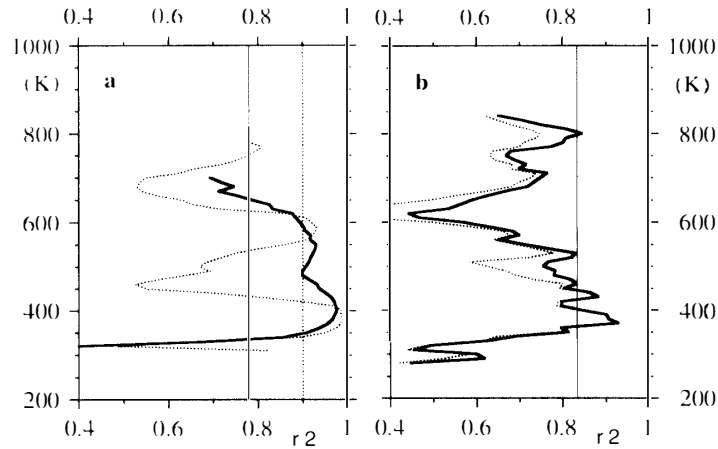


Fig. 1. Altitude distribution for  $r^2$  of multiple regression analysis according to eq. (1): (a) SY (spring) with  $T$ ,  $Q$ ,  $E$ ,  $S$  for the time interval 1966 to 1995 (solid line) and SY (spring) with  $T$ ,  $Q$ ,  $E$ ,  $S$ , and  $AE_{\text{tot}}$  for the time interval 1987 to 1995 (dotted line); (b) GFNM (October) with  $T$ ,  $Q$ ,  $E$ ,  $S$ , and  $AE_{\text{tot}}$  (solid line), and with  $T$ ,  $Q$ ,  $E$ ,  $S$  (dotted line); 95% confidence levels are indicated by vertical lines for each calculation; altitude coordinate is potential temperature.

Table 4. Sounding statistics of climatological means for three seasonally corresponding months and October: Georg Forster/Neumayer Stations (GFNM: 1985–1995) and Ny-Ålesund Station (NA: 1989–1995).

Antarctic		Arctic	
Month	GFNM (1985–1995)	Month	NA (1989–1995)
May	42/ 3 (1000 K)	November	46/ 4 (1000 K)
July	51/10 (1000 K)	January	86/ 9 (1000 K)
September	83/11 (1000 K)	March	118/33 (1000 K)
October	81/33 (1000 K)		

$x/y$  ( $z$ ) same as in Table 1.

to 1995 (KOENIG-LANGLO and HERBER, 1996). Furthermore climatological monthly means of the vertical ozone distribution were calculated for Antarctica by including data from GF and NM for the period from 1985 to 1995. For the Arctic 6-years (1989 to 1995) climatological means were obtained from ozone sonde data recorded at Ny-Ålesund (NA) ( $79^\circ\text{N}$ ,  $12^\circ\text{E}$ ). In Table 4 the contributing soundings are shown for seasonally corresponding months as May and November the time of vortex formation, July and January for winter season, and September and March for spring season. The recent mean annual variation of stratospheric ozone for both polar regions is also calculated by using balloon-borne ozone sounding data from 1992 to 1996 recorded at the Stations Neumayer (total 307 soundings) and Ny-Ålesund (total 537 soundings).

### 3. Results and Discussion on Trends in the Polar Stratosphere

The profiles for  $m_{1,i}$  (ppm/year) are shown in Fig. 2. For SY (spring) the trend coefficients  $m_{1,i}$  are different for the periods 1966 to 1995 and 1987 to 1995 (Fig. 2a). For the period 1966 to 1995 the partial correlation of trend is confident with 99% between 330 K and 670 K. But the confidence is less than 95% for the period 1987 to 1995. Both profiles clearly show the negative trends of stratospheric ozone for the SY (spring) means since 1966, *i.e.* a time interval of about 30 years. The trend is roughly twice as large between 400 K and 550 K than above 600 K with respect to the stratospheric ozone distribution 30 years ago. Since 1987 the ozone loss mainly continued between 500 K and 600 K as well as close to 400 K.

In Fig. 2b the GFNM (October) trend profile related to 1985 is compared with the SY (spring) trend profile related to 1987. Both profiles retrieved from independent data series are similar in their vertical structure but different in the trend rate. For GFNM (October) the retrieved trend rates (ppm/year) are stronger between 450 K and 600 K as well as above 700 K than those retrieved from the SY (spring) series. That suggests a stronger ozone decrease at these altitudes in October and a strengthening of the spring ozone minimum mainly due to the ozone losses between 500 K and 600 K. But negative trends have almost disappeared for both time series between 600 K and 700 K since the mid eighties.

One reason for the insufficient significance is the limited number of observations for the period 1985 to 1995. However, these trends should have some reliability, because similar results have been obtained for the two independent time series GFNM (October)

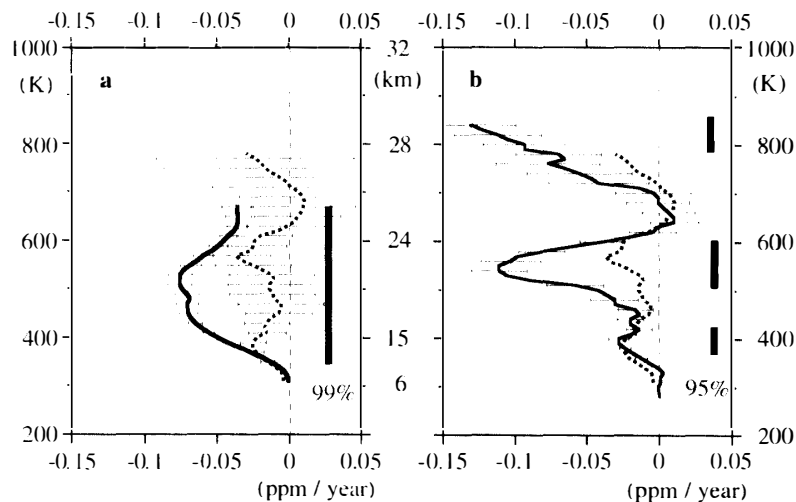


Fig. 2. Altitude dependent trends of ozone mixing ratio  $m_{1,i}$  (ppm/year); (a) for SY (spring) from 1966 to 1995 (solid line) with altitude range for 99% confidence and SY (spring) from 1987 to 1995 (dashed line); (b) for GFNM (October) from 1985 to 1995 (solid line) with altitude ranges for 95% confidence, and SY (spring) from 1987 to 1995 (dashed line); one standard deviation for  $m_{1,i}$  is shown for SY (spring) in (a) and for GFNM (October) in (b); altitude coordinate is potential temperature (K); approximate geopotential height (km) is also indicated.

and SY (spring) based on different means.

Because the GFNM (October) series shows the strongest trend signal with 95% confidence within three altitude ranges for the time interval from 1985 to 1995, these results are used to discuss altitude dependence of negative trend in more detail. The  $m_{1,i}$  profile for GFNM (October) shows three maxima with 95% confidence between 370 K and 390 K, 520 K and 590 K, and above 800 K (Fig. 2b). Since 1985 the negative trend has been small below 500 K because ozone was already completely removed at these altitudes in the mid eighties. But negative trends are identified above 500 K until 1995. Stratospheric temperatures were analysed for the period of stratospheric vortex existence by using all radiosonde observations recorded at NM for the period 1985 to 1995. For each isentropic level the absolute minimum temperatures and the first day of their appearance were selected for the winter-spring period, *i.e.* from May to October each year. At Fig. 3 the result is shown for three selected years for solar minimum 1985, for solar maximum 1991, and again for solar minimum 1995. Furthermore the temperature thresholds for the formation of typical PSC particles as NAT (nitric acid trihydrate) and water ice particles are shown in Fig. 3. These temperature thresholds were calculated by assuming a constant volume mixing ratio of 4.6 ppm by volume for H<sub>2</sub>O and a monthly zonal mean profile for HNO<sub>3</sub> retrieved from night-time LIMS data for January 1979 at 60° N (HANSON and MAUERSBERGER, 1988; WMO, 1991; VON DER GATHEN *et al.*, 1995).

In Fig. 3a it is seen that the altitude of minimum temperature significantly increases from 1985 to 1995. So the altitude range where polar stratospheric particles might be formed extended for ICE particles up to 600 K (24 km) and for NAT particles up to 700 K (26 km). Figure 3b shows that in the polar stratosphere these minimum tempera-

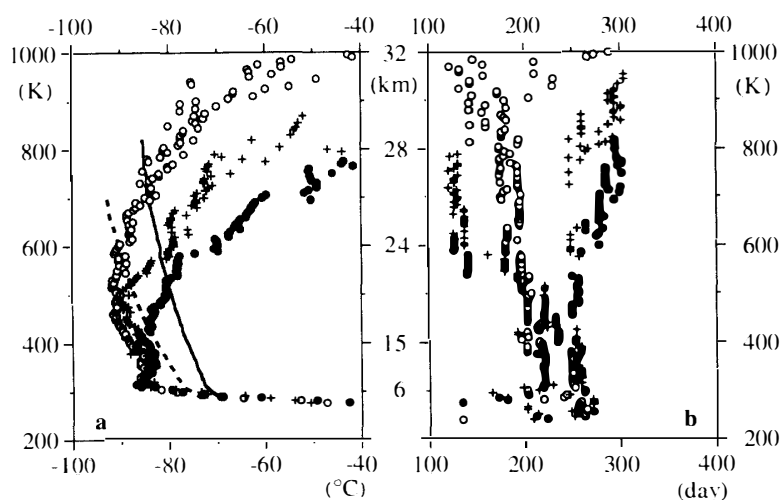


Fig. 3. Altitude distribution of minimum temperatures above NM between May and October for 1985 (solid circles), for 1991 (crosses), and for 1995 (open circles); (a) profiles of minimum temperatures ( $^{\circ}$ C) and temperature thresholds for nitric acid trihydrate (NAT) particle formation (solid line) and ice particle (ICE) formation (dashed line); (b) day of year when the minimum temperatures occurred; altitude coordinates are the same as in Fig. 2.

tures occurred by about 50 to 100 days earlier in 1995 than in 1985. Both the earlier appearance and vertical extension of sufficient low temperatures to form PSC particles may strengthen the chemical ozone loss even if the chemical composition would remain unchanged. In the lower polar stratosphere the net chemical ozone loss closely depends on the stability of the lower stratospheric vortex, the formation of different types of PSC particles below certain temperature thresholds, and subsequent heterogeneous activation of chlorine at the surface of these PSC particles. In that context the winter temperature history inside the stratospheric vortex is a necessary but not a sufficient condition for controlling the final total ozone depletion in October. The vertical extension of minimum temperature range within the polar stratospheric vortex in winter and spring from 1985 to 1995 are considered as a possible meteorological reason for the vertical extension of negative ozone trends up to 600 K. So the negative ozone trend between 500 K and 600 K altitude might be connected with changes in the occurrence of extremely low temperatures in winter and spring season.

This conclusion is supported by model calculations. AUSTIN and BUTCHERT (1992) have shown a dynamical coupling between the vertical extension of chemical ozone depletion inside the polar stratospheric vortex in spring and decreasing hemispheric planetary wave activity in the troposphere. Smaller tropospheric planetary wave amplitude yields to smaller forcing of diabatic downward motion of air inside the polar vortex and lower temperatures. So the vertical extension of chemical ozone losses up to 600 K might have a close and sensitive connection to global dynamical processes.

On the other hand below the 500 K level no significant change was observed for minimum temperatures with regard to the temperature threshold for PSC formation (Fig. 3a). Nevertheless ozone trends are still negative also at these altitudes (Fig. 2b). If the meteorological conditions and the formation of PSCs did not change significantly at these altitudes, the corresponding ozone trend might be accounted to growing levels of chlorine and bromine in the stratosphere due to the emission of CFCs and bromine compounds.

At altitudes above 700 K another negative ozone trend in ozone mixing ratio was found for both data series GFNM (October) and SY (spring) as seen in Fig. 2b. It is not likely that this ozone decrease is forced by the same chemical processes as in the lower stratosphere, because temperatures are not in the range to form additional PSCs as seen in Fig. 3a. But in the middle stratosphere negative trends were retrieved from combined Nimbus 7 SBUV and NOAA 11 SBUV/2 satellite data for mid and subpolar latitudes at 40 km altitude (HOOD and McCORMACK, 1992; HOLLANDSWORTH *et al.*, 1995). The strongest negative trend was found at subpolar latitudes in fall before the formation of the polar vortex. Because satellite observations are terminated to subpolar latitudes, a direct comparison with those inside the polar vortex is difficult. But we suggest a connection with the negative ozone trends identified by ozone sonde observations (Fig. 2b) in the middle stratosphere down to 26 km altitude inside the polar vortex with those retrieved from satellite observations for subpolar latitudes. Negative trends in the upper stratosphere at subpolar latitudes in fall might be extended down to the middle stratosphere inside the vortex until spring due to the diabatic downward motion of air during the vortex existence from fall to spring.

#### 4. Results and Discussion on Regular and Transient Forcing Processes

The altitude dependent correlation between ozone mixing ratio and the independent variables for QBO, ENSO, solar activity, and sulphate aerosols are discussed in detail for the period 1985 to 1995 with the results of the regression analyses for GFNM (October).

##### 4.1. Ozone forcing by QBO, ENSO, and solar activity for GFNM (October)

By using the corresponding regression coefficients ( $m_{n,i}$ ) and the values for the forcing variables (Table 3) the individual contributions are obtained as follows

$$\begin{aligned} \text{O3}_{2,i} (Q) &= m_{2,i} \times Q (t), \\ \text{O3}_{3,i} (E) &= m_{3,i} \times E (t), \\ \text{O3}_{4,i} (S) &= m_{4,i} \times S (t), \end{aligned} \quad (2)$$

where  $t$  is time in years from 1985 to 1995. The total ozone variability (O3 (sum)) incorporating forcing processes QBO, ENSO, and solar activity is then obtained by

$$\text{O3 (sum)} = \text{O3}_{2,i} (Q) + \text{O3}_{3,i} (E) + \text{O3}_{4,i} (S). \quad (3)$$

The interannual variability of  $\text{O3}_{n,i}$ , and O3 (sum) together with trends are shown for the isentropic levels 380 K, 530 K, 700 K, 800 K in Fig. 4. At these levels the confidence for  $r^2$  of the regression is about 95% (Fig. 1b).

The total variability in ozone mixing ratio increases with altitude. The amplitude of O3 (sum) is about 25% with respect to the climatological mean value at both upper levels. There the interannual variability of O3 (sum) is stronger than the trend. The ENSO signal shows the strongest interannual changes. At 800 K the ENSO amplitude is about 20% with respect to the climatological mean for October. The QBO and solar cycle signals amount less than 5%. At 380 K both the ENSO and QBO signals have similar small amplitudes but they are about 30% with respect to the climatological mean. The response to solar cycle is almost zero at the lowest level.

A synergetic effect is seen in the year to year variation of O3 (sum) if both the ENSO forcing and the QBO forcing are in phase, *i.e.*: easterly QBO winds coincide with positive SOI index values and *vice versa*. From 1985 to 1988 this in-phase forcing features the interannual change of ozone in the polar stratosphere at all selected altitude levels shown in Fig. 4. The strongest perturbations of polar stratospheric ozone in 1988 and 1992 are mainly related to the ENSO forcing.

The ozone response to the phase of mean QBO winds is similar at all selected altitudes. Higher ozone mixing ratios in the polar stratosphere appear during easterly QBO winds at 15 hPa. Because of the altitude dependent phase shift of QBO wind, mean westerly winds simultaneously appear at 50 hPa in this case. So the result shown here is also in general agreement with other studies mentioned in our introduction where the correlation between stratospheric ozone content and the phase of QBO wind has been analyzed for the 50 hPa level (LABITZKE, 1987).

The ozone response to solar activity is in opposite phase between 800 K (about 28 km) and 530 K (about 21 km). Higher ozone mixing ratios by about 0.25 ppm appear

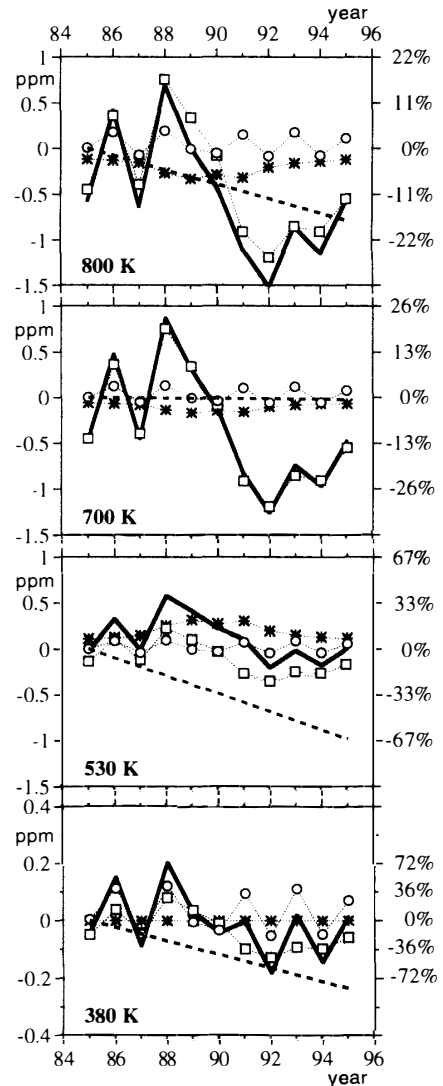


Fig. 4. Interannual variation of the total forcing  $O_3$  (sum) by QBO, ENSO, and solar cycle (solid bold line), and trend  $O_{3,1,i}$  ( $T$ ) (dashed bold line) for GFNM (October) at 800 K, 700 K, 530 K, and 380 K from 1985 to 1995; individual contributions ( $O_{3,n,i}$ ) to  $O_3$  (sum) for QBO as  $O_{3,2,i}$  ( $Q$ ) (dashed line with circles), ENSO as  $O_{3,3,i}$  ( $E$ ) (dashed line with squares), solar cycle as  $O_{3,4,i}$  ( $S$ ) (dashed line with asterisks); the ozone values are given in ppm (left scale) and % deviation from the climatological mean for October (right scale).

at 530 K during solar maximum from 1989 to 1991 (*cf.* Table 3). That is a change of about 13% with respect to the climatological mean. Lower mixing ratios by about  $-0.2$  ppm ( $-4\%$  to the climatological mean) are found for the middle stratosphere at 800 K. This different response by altitude might be explained by effects of solar energetic particles on the stratospheric composition, which result in transient ozone reductions in the middle polar stratosphere and also allow the solar UV flux to penetrate deeper into the lower stratosphere producing additional ozone there (ZEREFOS and CRUTZEN, 1975; JACKMAN *et al.*, 1990, 1995). The net effect of ozone reduction in the middle stratosphere is small and, therefore, can not be detected in column ozone analysis. But the increase of ozone as seen at 530 K where the maximum ozone concentration occurs in the polar stratosphere is in good agreement with modelled ozone column density variations by about  $-5\%$  from solar maximum to solar minimum due to the decrease of solar UV radiation (ZEREFOS *et al.*, 1997).

However, these signals are not found to be statistically significant for the partial correlations with 95% confidence at  $70^\circ\text{S}$  probably because they are masked by much

stronger natural variability having additional influence. So we can only show by these results a most likely teleconnection pattern between ozone in the polar stratosphere and forcing from outside.

#### 4.2. Transient perturbation by volcanic aerosols for GFNM (October)

After the Mt. Pinatubo and Cerro Hudson eruptions in 1991 volcanic aerosols were ejected into the stratosphere and rapidly distributed in a global scale (McCORMICK *et al.*, 1995). In September and October column aerosol surface densities significantly increased inside the southern polar vortex from 1991 to 1994 (Tables 2 and 3). The maximum perturbation occurred in 1992. In Fig. 5 zonally averaged mean vertical distributions of aerosol surface density ( $AE_{vol,i}$ ) for October 1992 are shown for three latitude belts at  $70 \pm 5^\circ S$ ,  $45 \pm 5^\circ S$ , and  $45 \pm 5^\circ N$ . For comparison the background state for October 1990 is also shown for  $70^\circ S$ . The  $AE_{vol,i}$  profiles were retrieved from SAGE II satellite observations of stratospheric aerosol extinction. In October 1992 increased aerosol concentrations were recorded below 22 km altitude inside the vortex. But in northern and southern mid-latitudes similar profiles with increased aerosol concentrations appear even up to 26 km altitude. This latitudinal difference in the vertical distribution is caused by the downward displacement of isolated vortex air from fall to spring.

The increased aerosol concentrations should have a direct impact on ozone in the polar stratosphere. The regression coefficients  $m_{5,i}$  for GFNM (October) were obtained by calculation (d). In order to get the corresponding ozone values as a function of the observed  $AE_{vol,i}$  profile, the column surface density  $AE_{tot}$  used in calculation (d) must be scaled to the altitude range where profiles for aerosol surface density ( $AE_{vol,i}$ ) and ozone mixing ratio ( $O_3_i$ ) were recorded. At  $70^\circ S$  this altitude range is located between 11.5 km to 23.5 km (Fig. 5). Above 23.5 km the aerosol surface density is almost zero, and below 11.5 km no data were obtained. By considering that the aerosol

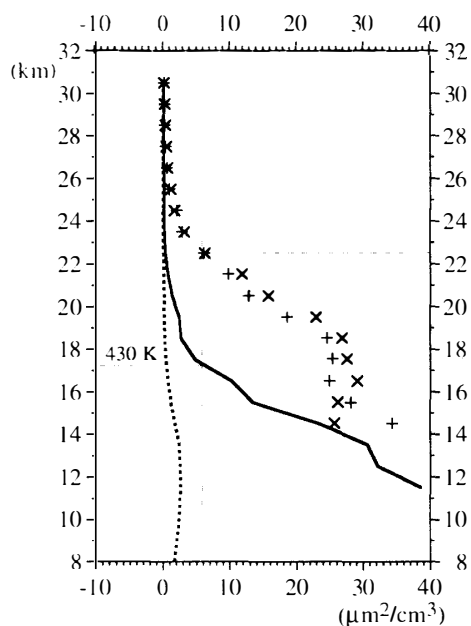


Fig. 5. Profiles of aerosol surface density  $AE_{vol,i}$  ( $\mu m^2/cm^3$ ) calculated as zonal means from SAGE II satellite data; October 1990 ( $65^\circ S - 75^\circ S$ ) (dotted line), October 1992 ( $65^\circ S - 75^\circ S$ ) (solid line), (+) October 1992 ( $45^\circ S - 55^\circ S$ ), and (x) October 1992 ( $45^\circ N - 55^\circ N$ ); horizontal scale is aerosol surface density ( $\mu m^2/cm^3$ ); altitude coordinate is geometric height (km).

column surface density  $AE_{\text{tot}}$  is related to the  $AE_{\text{vol},i}$  values as follows

$$AE_{\text{tot}} = \sum AE_{\text{vol},i} (\mu\text{m}^2/\text{cm}^3) \times h_i (\text{km}) = 176.8 (\mu\text{m}^2/\text{cm}^2).$$

The mean aerosol surface density by volume amounts

$$AE_{\text{vol}} (\text{mean}) = AE_{\text{tot}} / \sum h_i = 176.8 \mu\text{m}^2/\text{cm}^2 / 12 \text{ km} = 14.7 (\mu\text{m}^2/\text{cm}^3).$$

After the transformation of the geometric altitude scale (Fig. 5) to the potential temperature scale (Fig. 6a) the  $AE_{\text{vol},i}$  profile can be substituted for the  $AE_{\text{tot}}$  used in eq. (1). The ozone response for aerosol surface density  $AE_{\text{vol},i}$  at a certain isentropic level ( $i$ ) is then obtained by eq. (4).

$$O3_i (AE) = m_{s,i} \times AE_{\text{vol},i} \times (AE_{\text{tot}} / AE_{\text{vol}} (\text{mean})). \quad (4)$$

The result is shown in Fig. 6b.  $O3_i (AE)$  is positive above 430 K up to 550 K and negative below these heights. In the altitude range between 330 K and 350 K the partial correlation is even significant with 95% confidence. The maximum increase in ozone is roughly up to 0.15 ppm. The strongest decrease is roughly  $-0.2$  ppm in the

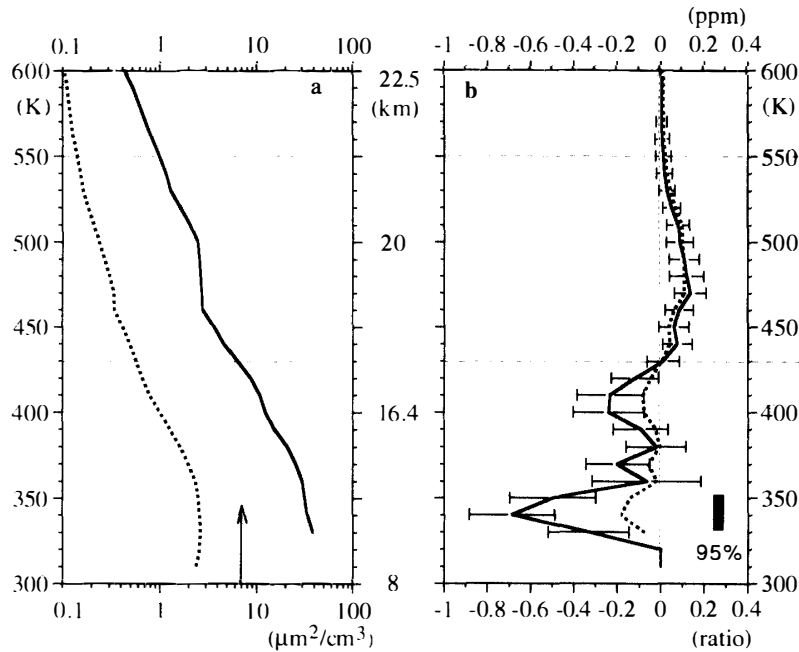


Fig. 6. (a) profiles of zonally averaged mean aerosol surface density  $AE_{\text{vol},i}$  ( $\mu\text{m}^2/\text{cm}^3$ ) for October 1990 (dotted line) and October 1992 (solid line); (b) profile of ozone amplitude ( $O3_i (AE)$  in ppm) for October 1992 (dotted line); profile of the  $O3_i (AE)$  ratio for October 1992 to climatological mean ozone profile for GFNM (October) from 1985 to 1995 (solid line); two standard deviations of  $m_{s,i}$  are indicated for the ozone ratio values; same scaling is used for ozone value (ppm) and ratio in the horizontal scale; altitude coordinates same as in Fig. 2.

layers directly located above the tropopause level at about 310 K. The ratio of these ozone values to the long-term climatological mean for October (Table 4) shows that ozone increases by about 10% at 470 K and decreases by about -20% around 400 K and by about -70% at 340 K, respectively.

The strong decrease of ozone mixing ratios obtained by the correlation analysis at the lowest stratospheric levels at 340 K for the time series GFNM (October) occurs where the aerosol loading is extremely high, *i.e.* greater than  $20\mu\text{m}^2/\text{cm}^3$  (Fig. 6). These ozone losses fairly well coincide with observations at South Pole Station in October 1992 (HOFMANN *et al.*, 1995) where also a strong decrease of ozone by -50% was recorded at altitudes between 10–14 km. Similar strong decreases of ozone in the lower stratosphere were found for Syowa Station in October 1992 (GERNANDT *et al.*, 1996). This connection of strong ozone losses with elevated concentration of volcanic aerosols in the lowest part of the stratosphere seems to be a typical feature for the polar region because such events were not reported by other observations performed in mid latitudes (*e.g.*, ANSMANN *et al.*, 1996).

Following the results of the regression analysis for GFNM (October) a reversal of ozone response to the additional aerosol loading is found at the 430 K level (about 17.5 km) inside the polar vortex (Fig. 6b). The reversal coincides with a “critical” aerosol surface density of about  $6\mu\text{m}^2/\text{cm}^3$  (Fig. 6a). However at mid latitudes the same “critical” aerosol surface density is found at altitudes of about 22.5 km (Fig. 5). So it is anticipated that the reversal of ozone response should be found at this altitude outside the vortex. Referring to the model results by TIE *et al.* (1994) a similar reversal altitude for ozone response at about 23 km was obtained at  $60^\circ\text{N}$  in March 1992 (*cf.* Fig. 14 of TIE *et al.*, 1994). TIE *et al.* (1994) also found an increase of ozone by about 10% above and an decrease by about 20% below this “critical” aerosol surface density. SOLOMON *et al.* (1996) also found additional ozone decrease for aerosol surface densities greater than about  $5\mu\text{m}^2/\text{cm}^3$  at altitudes below 25 km in mid latitudes.

With regard to the reversal altitude of ozone response these model results coincide very well with the correlation analysis based on the observations for GFNM (October) inside the southern stratospheric vortex. Because the “critical” aerosol surface density is shifted downward by about 5 km (Fig. 5), the same ozone response is found by our study inside the southern polar vortex. It might be concluded that similar chemical processes control ozone response above 380 K inside the vortex in October as in mid latitudes discussed in detail by TIE *et al.* (1994) and SOLOMON *et al.* (1996). But additional losses occur below 350 K in the polar stratosphere when the volcanic aerosol loading is extremely high. The chemical processes probably important for this removal of ozone are suggested by FAHEY *et al.* (1993).

## 5. Recent Stratospheric Ozone Distributions in the Antarctic and Arctic

Trends as well as forcing processes controlling the vertical distribution of ozone were studied for a small period of the year in the southern polar stratosphere. In Fig. 7 (upper and central panel) recent means of the annual ozone variation for the years 1992 to 1996 are shown for both polar regions above Neumayer Station ( $70^\circ\text{S}$ ,  $08^\circ\text{W}$ ) in the Antarctic and Ny-Ålesund Station ( $79^\circ\text{N}$ ,  $12^\circ\text{E}$ ) in the Arctic, respectively. The

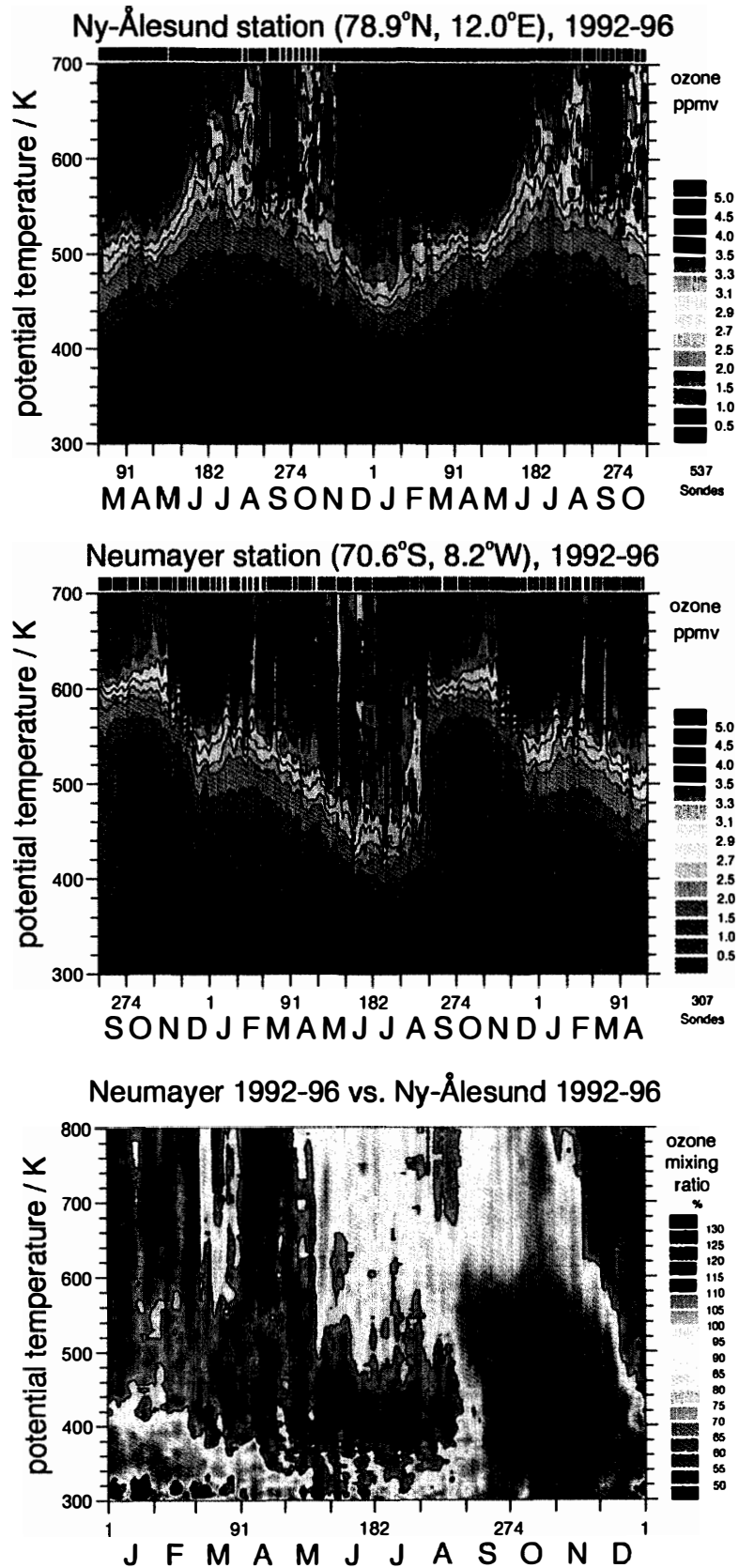


Fig. 7. Upper panel: height-time cross section of mean annual variation of ozone mixing ratio at Ny-Ålesund Station (79°N, 12°E) from 1992 to 1996 with 537 ozone soundings, color code is mixing ratio in ppm, time interval is 1.5 years scaled by day of year and months; central panel: same for Neumayer Station (70°S, 08°W) from 1992 to 1996 with 307 ozone soundings; lower panel: ratio (%) between Neumayer versus Ny-Ålesund for corresponding seasons, color code is % deviation (red indicates higher ozone mixing ratio in % at Neumayer than at Ny-Ålesund); time interval is one year scaled by day of year and months for Neumayer Station; altitude coordinate is potential temperature (K).

strong difference between both polar regions is evident for spring. In the Antarctic the spring ozone depletion is a striking feature. But recent analysis of coordinated ozone sonde observations have shown that chemical ozone loss also takes place in the Arctic stratosphere (VON DER GATHEN *et al.*, 1995; REX *et al.*, 1996). These ozone losses are also seen as a signature of slightly lower ozone mixing ratios up to 550 K in the mean annual variation for Ny-Ålesund from February until the middle of April. In the Arctic lower ozone mixing ratios appear in summer season from June until the formation of the wintery stratospheric vortex in November than in the Antarctic for the same season.

The seasonal differences between both polar records are demonstrated in detail by taking the ratio of mean annual variations for corresponding seasons in Fig. 7 (lower panel), *i.e.* Neumayer *versus* Ny-Ålesund. In the Antarctic stratosphere the mean ozone mixing ratios are higher above 600 K in the middle stratosphere during summer and fall and between 400 K and 500 K in the lower stratosphere during winter. Lower mean ozone mixing ratios occur up to 600 K in spring. In the lowest part of the stratosphere between 300 K and 400 K ozone mixing ratios remain low until summer.

Finally some features of similarity between Antarctic and Arctic mean annual variations are shown in Fig. 8. This intercomparison is made by using climatological monthly means for May, July, and September in Antarctica from 1985 to 1995, *i.e.* all available data from Stations Georg Forster and Neumayer (GFNM), and for corresponding seasonal months November, January, and March in the Arctic from 1989 to 1995, *i.e.* data from Ny-Ålesund (NA) Station (Table 4).

In Fig. 8a differences in the ozone mixing ratio are shown for July minus May for the Antarctic and January minus November for the Arctic, respectively. Ozone mixing ratios increase in both polar regions by about 1 ppm during winter season from May to

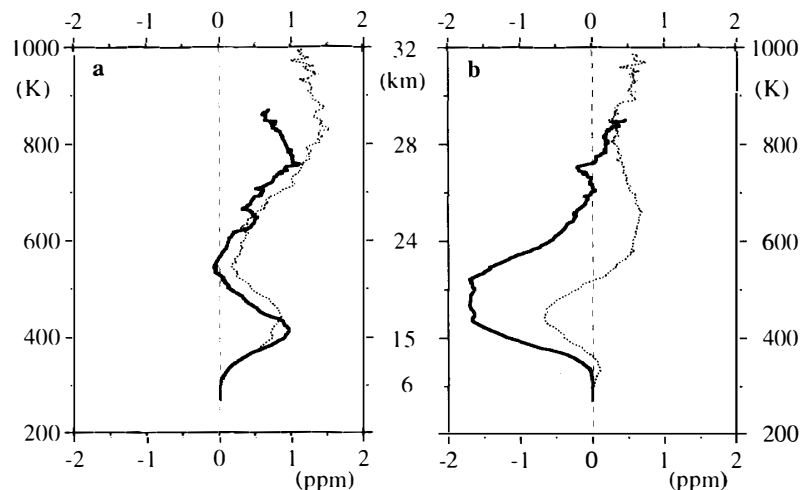


Fig. 8. Mean seasonal variation of ozone mixing ratios (ppm) at isentropic levels for Antarctica at 70°S (solid lines) and for Arctic at 79°N (dotted lines): (a) polar night net change (July minus May for Antarctica and January minus November for the Arctic), (b) late winter net change (September minus July for Antarctica, and March minus January for the Arctic); altitude coordinates same as in Fig. 2.

July as well as from November to January, respectively. This similar net ozone change for both polar regions is identified for two separated altitude ranges. Almost no change is found between 500 K and 600 K. Despite of the differences in the mean annual variation as shown in Fig. 7, similarities can be recognized in the seasonal changes from fall to spring. It is suggested that the stronger ozone increase in the Arctic from January to March is caused by the well known dynamical perturbations of the stratospheric vortex. From January until March ozone continues to increase by about 0.5 ppm above 500 K in the Arctic and above 700 K for corresponding months in the Antarctic (Fig. 8b). But ozone decreases below these altitudes in both polar regions. This net ozone loss is stronger in the Antarctic. Low ozone mixing ratios are extended over a greater altitude range. At 420 K the Arctic ozone loss amounts about 30% of that recorded in the Antarctic.

The intercomparison of recent balloon-borne ozone observations in the Arctic and Antarctica from 1992 to 1995 shows significant differences in the mean annual pattern but also similarities in the seasonal behaviour. Late winter differences between both polar regions are also attributed to a different dynamical forcing in both hemispheres.

## 6. Conclusion

This attempt to assess the interannual variability of ozone inside the southern polar vortex by balloon-borne ozone sonde data recorded at three Antarctic stations located at around 70°S between 30°E and 8°W is focused to spring season. It shows the importance of meteorological conditions in the polar stratosphere as well as global forcing processes on the PSC related chemical ozone loss in the southern polar stratosphere.

For the last solar cycle three altitude ranges with significant negative trends were found for GFNM (October). The trends above 500 K are similar in their loss rates and roughly three times stronger than the trend in the lower stratosphere below the 500 K level. The continued ozone loss in the lower stratosphere below 500 K might be directly connected with the continued elevation of chlorine and bromine compounds. But at both upper levels, although the ozone loss processes are basically different between these levels, there are indications for primary dynamical causes of strong negative trends since 1985.

The discussed correlations with QBO, ENSO, and solar activity do not explain the nature of dynamical processes being responsible for these teleconnections between polar stratospheric ozone and forcing processes outside the polar stratosphere. But it seems to be most likely that the El Niño Southern Oscillation has a dominating impact on ozone content in the polar middle stratosphere. The interannual variation of stratospheric ozone from 1985 to 1988 might reasonably be explained by a synergetic effect of in-phase interannual variations of ENSO and QBO winds at 15 hPa. However, these signals are not found to be statistically significant at all altitudes probably because of additional influences not considered in the analysis. The impact of global atmospheric variability on polar stratospheric ozone is extremely complicated and can probably not be understood in all details by simple linear regression analysis to QBO, ENSO, or solar activity.

Transient perturbations by volcanic aerosols may also change the vertical ozone distribution inside the polar vortex. Although the retrieved correlation between ozone and volcanic aerosols loading is also not significant with 95% confidence, a general good agreement was found between observations inside the polar vortex and model results for lower latitudes at altitudes above 15 km. Below this altitude, near the tropopause, the strongest response with ozone losses by about  $-70\%$  was found with 95% confidence.

The intercomparison of stratospheric ozone distributions between the Arctic and the Antarctic indicates similar seasonal variability despite of differences in the ozone abundance at different altitudes.

The long-term variability of stratospheric ozone, the impact of volcanic aerosols as well as global forcing processes as a function of altitude needs further detailed analysis of temperature and ozone records from both polar regions for all seasons of the year.

### Acknowledgments

The performance of regular observations at the polar stations Syowa, Georg Forster, and Neumayer is gratefully credited to all staff members having contributed data for this study. Thanks are to Larry THOMASON from NASA Langley Research Center, Hampton, for providing SAGE II data for retrieving the vertical distribution of aerosol surface area densities for the period 1985 to 1995, to Barbara NAUJOKAT and Karin LABITZKE from the Free University of Berlin for providing updated 10.7 cm solar radio flux and QBO data, to Phil JONES from the Climate Research Unit of the University of East Anglia, Norwich, for providing the SOI index data, and last but not least to Gert KÖNIG-LANGLO from the Alfred Wegener Institute for Polar and Marine Research for helpful assistance to retrieve radiosonde data of Neumayer Station from the MISAWI database.

AWI contribution number: 1284.

### References

- ANGEL, J.K. (1988): Variations and trends in tropospheric and stratospheric global temperatures, 1958–87. *J. Clim.*, **1**, 1296–1313.
- ANGEL, J.K. (1989): On the relation between atmospheric ozone and sunspot number. *J. Clim.*, **2**, 1404–1416.
- ANSMANN, A., WAGNER, F., WANDINGER, U., MATTIS, I., GÖRSDORF, U., DIER, H.-D. and REICHARDT, R. (1996): Pinatubo aerosol and stratospheric ozone reduction: Observations over central Europe. *J. Geophys. Res.*, **101**, 18775–18785.
- AUSTIN, J. and BUTCHERT, N. (1992): A three-dimensional modeling study of the influence of planetary wave dynamics on polar ozone photochemistry. *J. Geophys. Res.*, **97**, 10165–10186.
- BOJKOV, R.D. and FIOLETOV, V.E. (1995): Estimating the global ozone characteristics during the last 30 years. *J. Geophys. Res.*, **100**, 16537–16551.
- BOWMAN, K.P. (1989): Global patterns of the quasi-biennial oscillation in total ozone. *J. Atmos. Sci.*, **46**, 3328–3343.
- CLAUDE, H., SCHÖENENBORN, F., STEINBRECHT, W. and VANDERSEE, W. (1994): New evidence for ozonier depletion in the upper stratosphere. *Geophys. Res. Lett.*, **21**, 2409–2412.
- CHUBACHI, S. (1984): Preliminary result of ozone observations at Syowa from February 1982 to January 1983. *Mem. Natl. Inst. Polar Res., Spec. Issue*, **34**, 13–19.
- CHUBACHI, S. (1993): Relationship between total ozone amounts and stratospheric temperatures at Syowa, Antarctica. *J. Geophys. Res.*, **98**, 3004–3010.

- FAHEY, D.W., KAWA, S.R. and WOODBRIDGE, E.L. (1993): In situ measurements constraining the role of sulphate aerosols in mid-latitude ozone depletion. *Nature*, **363**, 509–514.
- GERNANDT, H., HERBER, A., VON DER GATHEN, P., REX, M., RINKE, A., WESSEL, S. and KANETO, S. (1996): Variability of ozone and aerosols in the polar atmosphere. *Mem. Natl Inst. Polar Res., Spec. Issue*, **51**, 189–215.
- GRUDZEV, A.N. and MOKHOV, I.I. (1992): Quasi-biennial oscillation in the total ozone global field from ground based observations. *Isv. Atmos. Ocean. Phys.*, **28** (5), 358–366.
- HANSON, D. and MAUERSBERGER, K. (1988): Laboratory studies of the nitric acid trihydrate: Implications for the south polar stratosphere. *Geophys. Res. Lett.*, **15**, 855–858.
- HASEBE, F. (1980): A global analysis of the fluctuations in total ozone, II. Nonstationary annual oscillation, quasi-biennial oscillation, and long-term variations in total ozone. *J. Meteorol. Soc. Jpn.*, **58**, 104–117.
- HOFMANN, D.J. and OLTMANS, S.J. (1993): Anomalous Antarctic ozone during 1992: Evidence for Pinatubo volcanic aerosol effects. *J. Geophys. Res.*, **98**, 18555–18561.
- HOFMANN, D.J., OLTMANS, S.J., LATHOP, J.A., HARRIS, J.M. and VOMEL, H. (1994): Record low ozone at the South Pole in spring of 1993. *Geophys. Res. Lett.*, **21**, 421–424.
- HOFMANN, D.J., OLTMANS, S.J., LATHOP, J.A., HARRIS, J.M. and VOMEL, H. (1995): Recovery of ozone in the lower stratosphere at the South Pole during the spring of 1994. *Geophys. Res. Lett.*, **22**, 2493–2496.
- HOLLANDSWORTH, S.M., MCPETERS, R.D., FLYNN, L.E., PLANET, W., MILLER, A.J. and CHANDRA, S. (1995): Ozone trends deduced from combined Nimbus 7 SBUV and NOAA 11 SBUV/2 data. *Geophys. Res. Lett.*, **22**, 905–908.
- HOOD, L.L. and McCORMACK, J.P. (1992): Components of interannual ozone change based on Nimbus 7 TOMS data. *Geophys. Res. Lett.*, **19**, 2309–2312.
- HOOD, L.L., MCPETERS, R.D., McCORMACK, J.P., FLYNN, L.E., HOLLANDSWORTH, S.M. and GLEASON, J. F. (1993): Altitude dependence of stratospheric ozone trends based on NIMBUS 7 SBUV data. *Geophys. Res. Lett.*, **20**, 2667–2670.
- JACKMAN, C.H., DOUGLASS, A.R., ROOD, R.B., MCPETERS, R.D. and MEADE, P.E. (1990): Effect of solar proton events on the middle atmosphere during the past two solar cycles using a two-dimensional model. *J. Geophys. Res.*, **95**, 7417–7428.
- JACKMAN, C.H., VITT, F.M., CONSIDINE, D.B. and FLEMING, E. (1995): Energetic particle precipitation effects on stratospheric odd nitrogen and ozone on the solar cycle time scale. Presented at the International Union of Geodesy and Geophysics XXI General Assembly, Boulder, Colorado.
- JOHNSON, B.J., DESHLER, T. and ZHAO, R. (1995): Ozone profiles at McMurdo Station, Antarctica during the spring of 1993; Record low ozone season. *Geophys. Res. Lett.*, **22**, 183–186.
- KÖENIG-LANGLO, G. and HERBER, A. (1996): The meteorological data of Neumayer Station (Antarctica) for 1992, 1993, and 1994. *Ber. Polarforsch. (Rep. Polar Res.)*, **187**, 101 p.
- LABITZKE, K. (1987): Sunspots, the QBO, and stratospheric temperature in the north polar region. *Geophys. Res. Lett.*, **14**, 535–537.
- McCORMICK, P.M., THOMASON, L.W. and TREPTE, Ch.R. (1995): Atmospheric effects of the Mt. Pinatubo eruption. *Nature*, **373**, 399–404.
- RANDEL, W.J. and COBB, J.B. (1994): Coherent variations of monthly mean total ozone and lower stratospheric temperature. *J. Geophys. Res.*, **99**, 5433–5447.
- REX, M. *et al.* (1996): Chemical ozone loss in the Arctic Winters 1991/92 and 1994/95 (Match). *Polar Stratospheric Ozone: Proceedings of the Third European Workshop 18 to 22 September 1995 Schliersee, Bavaria, Germany*, ed. by J.A. PYLE *et al.* (Air Pollution Research Report, 56) (ISBN 92-827-5722-6).
- SHIOTANI, M. (1992): Annual, quasi-biennial, and El Nino-Southern Oscillation (ENSO) timescale variations in equatorial total ozone. *J. Geophys. Res.*, **97**, 7625–7633.
- SOLOMON, S. (1990): Progress towards a quantitative understanding of Antarctic ozone depletion. *Nature*, **347**, 347–353.
- SOLOMON, S., PORTMANN, R.W., GARCIA, R.R., THOMASON, L.W., POOLE, L.R. and McCORMICK, M.P. (1996): The role of aerosol variations in anthropogenic ozone depletion at northern midlatitudes. *J.*

- Geophys. Res., **101**, 6713–6727.
- STOLARSKI, R., BOJKOV, R.D., BISHOP, L., ZEREFOS, C., STAEHELIN, J. and ZAWODNY, J. (1992): Measured trend in stratospheric ozone. *Science*, **256**, 342–349.
- TAUBENHEIM, J. (1969): Statistische Auswertung geophysikalischer und meteorologischer Daten. Akademische Verlagsgesellschaft Geest & Portig K.-G., VLN 276–105/7/69 ES 18 E 1, Leipzig.
- TIE, X. Xi, BRASSEUR, G.P., BRIEGLEB, B. and GRANIER, C. (1994): Two dimensional simulation of Pinatubo aerosol and its effect on stratospheric ozone. *J. Geophys. Res.*, **99**, 20545–20562.
- VAN LOON, H. and LABITZKE, K. (1990): Association between the 11-year solar cycle and the atmosphere, IV. The stratosphere, not grouped by the phase of the QBO. *J. Clim.*, **3**, 827–837.
- VON DER GATHEN, P., REX, M., HARRIS, N.R.P., LUCIC, D., KNUDSEN, B.M. *et al.* (1995): Observational evidence for chemical ozone depletion over the Arctic in winter 1991–92. *Nature*, **375**, 131–134.
- WMO (World Meteorological Organization) (1991): Scientific Assessment of Ozone Depletion: 1991. WMO, Global Ozone Research and Monitoring Project - Report No. 25.
- WMO (World Meteorological Organization) (1994): Scientific Assessment of Ozone Depletion: 1994. WMO, Global Ozone Research and Monitoring Project - Report No. 37.
- ZEREFOS, C.S. and CRUTZEN, J.P. (1975): Stratospheric thickness variations over the northern hemisphere and their relation to solar activity. *J. Geophys. Res.*, **80**, 5041–5043.
- ZEREFOS, C.S., BAIS, A.F., ZIOMAS, I.C. and BOJKOV, R.D. (1992): On the relative importance of quasi-biennial oscillation and El Niño/Southern Oscillation in the revised Dobson total ozone records. *J. Geophys. Res.*, **97**, 10135–10144.
- ZEREFOS, C.S., TOURPALI, K., BOJKOV, B.R., BALIS, D.S., ROGNERUND, B. and ISAKSEN, I.S.A. (1997): Solar activity-total column ozone relationships: Observations and model studies with heterogeneous chemistry. *J. Geophys. Res.*, **102**, 1561–1569.

*(Received April 14, 1997; Revised manuscript accepted October 20, 1997)*